

# Design, Fabrication and Testing of Integrated Nano-Scale Vibration-Based Prototype Model of Electromagnetic Generator

<sup>[1]</sup>Antonio Dias,<sup>[2]</sup>Jeevesh Jadhav,<sup>[3]</sup>Rachana Chougule,<sup>[4]</sup>Sangeeta M Raibagi  
<sup>[1][2][3][4]</sup>UG Students, Department of Electrical & Electronics Engineering,  
VTU, Belagavi

<sup>[1]</sup>tonydias007@gmail.com,<sup>[2]</sup>jadhavjeevesh@gmail.com,<sup>[3]</sup>rachanachougule149@gmail.com,<sup>[4]</sup>sangeetaraibagi149@gmail.com

**Abstract**— This paper discusses the design, fabrication and testing of electromagnetic nanogenerators. Three different designs of power generators are partially nano-fabricated and assembled. Prototype A having a wire-wound copper coil, Prototype B, an electrodeposited copper coil both on a deep reactive ion etched (DRIE) silicon beam and paddle. Prototype C uses moving NdFeB magnets in between two nano-fabricated coils. The integrated coil, paddle and beam were fabricated using standard Nano-electro-mechanical systems (NEMS) processing techniques. For Prototype A, the maximum measured power output was 148nW at 8.08 kHz resonant frequency and 6.8 m/s<sup>2</sup> acceleration. For Prototype B, the nano generator gave a maximum load power of 23nW for an acceleration of 9.8 m/s<sup>2</sup>, at a resonant frequency of 18.83 kHz. This is a substantial improvement in power generated over other nano-fabricated silicon-based generators reported in literature. This generator has a volume of 0.1 cm<sup>3</sup> which is lowest of all the silicon-based nano-fabricated electromagnetic power generators reported. To verify the potential of integrated coils in electromagnetic generators, Prototype C was assembled. This generated a maximum load power of 586nW across 110 load at 60 Hz for an acceleration of 8.829 m/s<sup>2</sup>.

**Keywords**— Energy harvesting from vibrations; Nano-fabricated electromagnetic power generator; NEMS fabrication techniques; Testing of power generator

## I. INTRODUCTION

Recently, energy harvesting has emerged as a solution for powering autonomous sensor nodes to increase their expected lifetimes. In wireless sensor applications where photovoltaic, optical, thermal, or electrical energy sources are not practical or available, energy harvesting devices that convert kinetic energy into electrical energy have attracted much interest. A variety of nano-machined vibration driven generators using electromagnetic principles to convert the kinetic energy of a suspended mass into electrical energy, are being studied for powering wireless sensor nodes. With the decreasing size and power requirements of wireless sensor networks, there exists a significant driver to miniaturize the size of the power generators.

Beeby et al. [1] have made a detailed review of the state of the art of vibration powered generators. Here, we briefly review the main results relating to electromagnetic devices. In their recent work, Beeby et al. [2], present working of a small (volume 0.1 cm<sup>3</sup>) electromagnetic generator using moving NdFeB magnets on beryllium copper beam, placed around a fixed wire wound coil. They reported a maximum power at the intensity of 46 W from the device in a 6 k load from 0.59 m/s<sup>2</sup> acceleration at a resonant frequency of 52 Hz. Previously, El Hami et al. [3] presented results from an electromagnetic power generator comprising of cantilever beam with a pair of NdFeB

magnets with wire-wound coil fixed between the poles of the magnets. They reported 1mW of power generated for a 0.29 cm<sup>3</sup> volume at a frequency of 320 Hz. Further, Glynne-Jones et al. [4] demonstrated working of an assembled electromagnetic power generator, using fixed bulk magnets and moving wire-wound coil fixed on a stainless steel beam. The generator produced a power of 180 W at a frequency of 322 Hz, acceleration of 2.7 m/s<sup>2</sup> and had a volume of 0.84 cm<sup>3</sup>. In recent work, Serre et al. [5] used a moving NdFeB magnet on a polyamide film and a fixed planar coil made of aluminum layer. The device produced a power of 200nW at a resonant frequency of 360 Hz for a displacement of 6.8m.

In other work, Mizuno et al. [6] described the use of an integrated coil on a cantilever beam with fixed NdFeB magnets. They predicted a maximum power of 0.4nW for a volume of 2.6 cm<sup>3</sup> at a frequency of 700 Hz and acceleration of 12.4 m/s<sup>2</sup>. A silicon-based generator was reported by Kulah and Najafi [7], comprising of two separated chips combined together. They reported a maximum power of 4nWatt 25Hz frequency and volume of 2 cm<sup>3</sup>. The review by Beeby et al. [1] shows that there are no reported fully nano-fabricated (i.e., nano-fabricated coils, magnets, beam and housing) electromagnetic vibration generators to-date. The silicon-based nano-fabricated generators have low coil turns compared to the discretely

assembled generators. Hence, a lower generated voltage and power when compared to discretely assembled devices. In order to compensate for low coil turns, we designed the generator to work at high frequencies. Here, the power generators were designed to work at input resonant frequency of 7400 Hz and acceleration of 1.1 m/s<sup>2</sup>. These values were measured in commonly used industrial fan. In this case, vibrations are induced from rotating parts that may be improperly balanced. In our previous works [8], we have reported the design, simulation and assembly process of a nanogenerator using integrated coils on silicon with NdFeB bulk magnets. For further integration, cost reduction and batch fabrication of the electromagnetic generator [9], we have reported the simulation results for a generator using integrated coils and electroplated CoPt nano-magnets. In our recent work, we suggest a novel method of developing nanostructured, stress-free and thick Co-rich CoPtP films using a combination of pulse-reverse plating and addition of stress relieving additives [10].

In this paper, we report further on a nano-scale vibration powered generator fabricated with an integrated Cu-coil (electroplated) on silicon and bulk NdFeB magnets. We discuss the design, fabrication and assembly of three different electromagnetic generators. Prototypes A and B use wire-wound and electroplated coils, respectively, on a DRIE etched silicon paddle. The coils are placed between two sets of oppositely polarized NdFeB magnets. The volume of both the devices was around 106mm<sup>3</sup>. It was observed that Prototypes A and B generated lower power output than expected. This was due to large parasitic damping in the silicon beam which reduced the amplitude of vibration leading to low power output. In order to verify the functioning of the integrated coils in the power generator a new design, Prototype C, comprising of fixed integrated coil on silicon and two oppositely polarized NdFeB magnets placed above and below a beryllium-copper beam was assembled. This design had a lower parasitic damping, allowing the beryllium-copper beam and the magnets to vibrate with higher amplitudes. This device has a component volume of 150mm<sup>3</sup>. Here, we compare the performance and characteristics of the three different power generators.

## II. FABRICATION AND ASSEMBLY PROCESS

The electromagnetic power generators work on the principle of electromagnetic induction. According to Faraday's law any time change in the magnetic field linking a coil will cause a voltage to be induced in the coil. The change could be produced either by moving the magnet,

while keeping the coil fixed or vice versa. In this work, Prototypes A and B have fixed magnets with moving coils, while Prototype C uses fixed coils and moving magnets. The design, modeling and simulation details of the Prototypes A & B have been reported previously [8]. Fig. 1 shows the schematic of the assembled power generator for Prototypes A & B.

In this work, we use wire-wound Cu coils, thereby realizing a partially batch-fabricated version (Prototype A) and electroplated Cu coils, as a fully batch fabricated version (Prototype B). In both cases the coils are placed on a DRIE etched vibrating silicon paddle. Both devices use a soft magnetic steel plate over the hard magnets to concentrate the flux lines. In our previous work [9], we have shown that the output power generated can be improved by using a soft magnetic layer to concentrate the flux lines in the region between the magnets. Prototype C comprises sintered NdFeB magnets and beryllium-copper beam with integrated coils fabricated through standard NEMS processing techniques. Fig. 2 shows the schematic for Prototype C. For the three devices, the arrangement of magnets with the coils is such that each magnet covers half of the coils. The advantage of this arrangement is to maximize the flux gradient by vibrating the coils from a region of positive flux to negative flux. Fabrication details of Prototype A have been described previously [11].

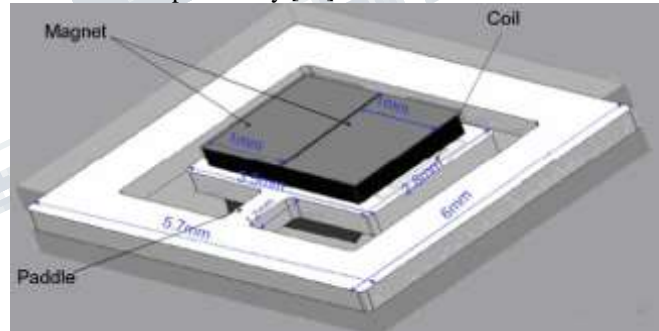


Fig. 1. Schematic electromagnetic power generator Prototype A & B.

Prototype A & B, use a moving silicon paddle with Cu coils in a magnetic field for power generation. Four-inch silicon wafers with high resistivity (21–33cm) were etched by a DRIE process to fabricate the silicon paddle, frame and beam. Here, we spin and pattern a 20m thick SPR220 resist and DRIE etch the silicon through the wafer. As a first test of the mechanical strength, the paddle and beam were tested using a standard weight set gradually added to a thin wire attached across the paddle. The weight was increased until the silicon structure broke. This simple test showed that the silicon beam could withstand 2.8–3N applied force without and 4.5–5.5N after chemical polishing.

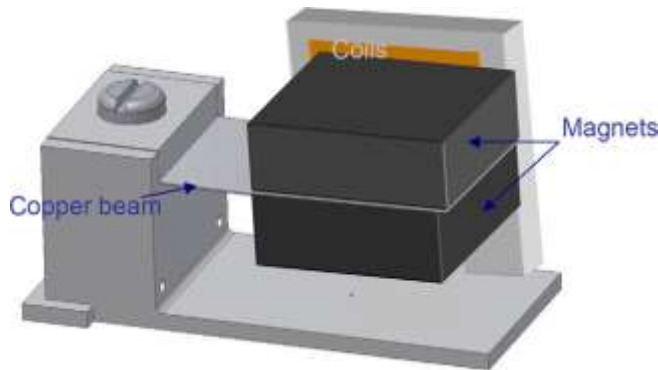


Fig. 2. Schematic of electromagnetic power generator Prototype C.

Prototype A uses a conventionally wound coils with 600 turns, of 25  $\mu$ m diameter enameled copper wire recessed in a silicon cantilever paddle. The coil internal diameter is 0.5 mm, external diameter is 2.4mm and a thickness is 0.5 mm. The measured resistance of the coil was 112. The resulting mass of the silicon paddle plus coil was 0.028 g. In Prototype B, the wire wound copper coil is replaced by an electroplated copper coil. The basic electroplated coil design is a square, spiral structure with a 150 $\mu$ m contact pad in the centre. The coils have a track width and track space of 10 $\mu$ m with 65 turns and a coil resistance of 55. The 10 $\mu$ m thick copper coils are electrodeposited on top of an insulated 2 $\mu$ m thick bottom copper layer, which is sputtered on a silicon paddle (3.5mm $\times$ 2.8mm $\times$ 0.5 mm). The paddle is etched by DRIE and batch fabricated on a silicon wafer. A silicon cantilever beam (0.3mm $\times$ 1.2mm $\times$ 0.5 mm) connects the paddle to the frame. The mass of the silicon paddle with coil was 0.014 g. Fig. 3 shows the process steps involved in the fabrication of an integrated coil on a DRIE etched paddle. Fig. 4 shows the resulting electrodeposited coil structure on a DRIE etched silicon paddle.

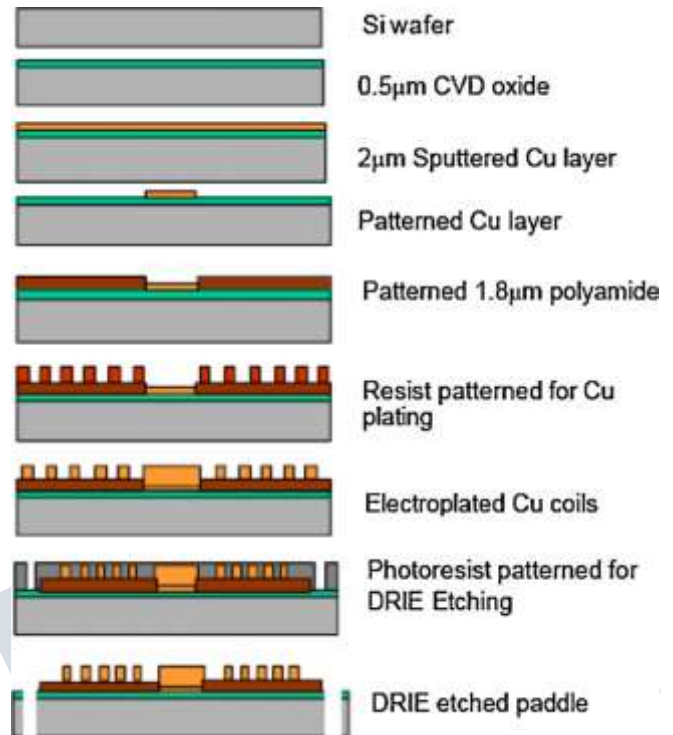


Fig. 3. Overview of process steps for integrated coil fabrication.

For final assembly of Prototype A & B, the integrated coil (wire-wound and electroplated coils on silicon) is bonded between two sets of oppositely polarized NdFeB magnets, assembled in a Perspex chip. For the magnet assembly, Perspex chips (6mm $\times$ 6mm $\times$ 3 mm) are fabricated using traditional milling techniques. Each chip has a (2mm $\times$ 2mm $\times$ 2 mm) cavity etched in the middle. A steel plate (2mm $\times$ 1mm $\times$ 1 mm) is glued in the Perspex etched slot, over which two oppositely polarized NdFeB magnets (1mm $\times$ 2mm $\times$ 1mm) are bonded. Two such Perspex chips containing the magnets are individually glued on the silicon chip with DRIE etched paddle. During assembly, the three chips are placed such that the magnets are aligned over center of the coil. Fig. 5 shows the SEM image of a DRIE etched silicon paddle with a recess for wire-wound coil (Prototype A). The assembled nanogenerator with discrete magnets and integrated coil is shown in Fig. 6.

Prototype C uses two bulk NdFeB magnets (3mm $\times$ 1mm $\times$ 1.5 mm). One magnet is placed above and the other with opposite polarity, below a beryllium/copper beam, which is 9mm long, 3mm wide and 55 $\mu$ m thick. The cantilever beam assembly was clamped onto the base using an M1 sized nut, bolt and a washer. The mass of the beam with the magnets was 0.54 g. Two of the above electroplated

Cu coils on silicon were fixed on either side of the magnets and the beam. The number of turns in a single coil was 65 and coil resistance of each integrated coil was measured to be 55. Hence, the total coil Fig. 3. Overview of process steps for integrated coil fabrication.

For final assembly of Prototype A & B, the integrated coil (wire-wound and electroplated coils on silicon) is bonded between two sets of oppositely polarized NdFeB magnets, assembled in a Perspex chip. For the magnet assembly, Perspex chips (6mm×6mm×3 mm) are fabricated using traditional milling techniques. Each chip has a (2mm×2mm×2 mm) cavity etched in the middle. A steel plate (2mm×1mm×1 mm) is glued in the Perspex etched slot, over which two oppositely polarized NdFeB magnets (1mm×2mm×1mm) are bonded. Two such Perspex chips containing the magnets are individually glued on the silicon chip with DRIE etched paddle. During assembly, the three chips are placed such that the magnets are aligned over center of the coil. Fig. 5 shows the SEM image of a DRIE etched silicon paddle with a recess for wire-wound coil (Prototype A). The assembled nanogenerator with discrete magnets and integrated coil is shown in Fig. 6.

Prototype C uses two bulk NdFeB magnets (3mm×1mm×1.5 mm). One magnet is placed above and the other with opposite polarity, below a beryllium/copper beam, which is 9mm long, 3mm wide and 55µm thick. The cantilever beam assembly was clamped onto the base using an M1 sized nut, bolt and a washer. The mass of the beam with the magnets was 0.54 g. Two of the above electroplated Cu coils on silicon were fixed on either side of the magnets and the beam. The number of turns in a single coil was 65 and coil resistance of each integrated coil was measured to be 55. Hence, the total coil

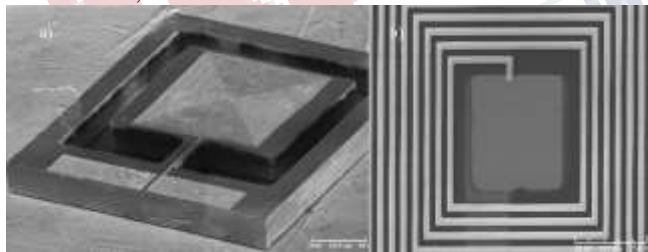


Fig.4. SEM image of (a) integrated coil structure with DRIE etched paddle and (b) electroplated copper coil structure.

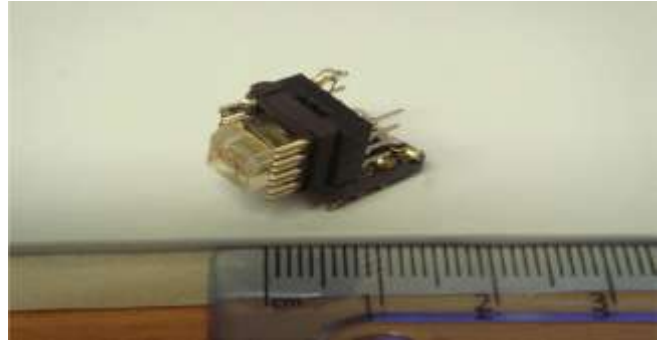


Fig. 6. Assembled silicon generator, Prototype A & B with discrete magnets and integrated coils

### III. RESULTS AND DISCUSSION

For measurement of generator output power, the two Prototypes were tested using a Bruel & Kjaer 4810 mini shaker driven from a signal generator through a power amplifier. The excitation vibrations were measured using a Piezotronics (model 354C03) three-axis accelerometer. The tests were performed at acceleration levels of 3.924 m/s<sup>2</sup> for Prototype A and 9.81–39.24 m/s<sup>2</sup> for Prototype B device. The resonant frequencies of the two generators were measured on a Hewlett Packard 3588 A 10Hz to 150MHz spectrum analyzer. The generator output was applied across an impedance matched load and the voltage was observed on a digital oscilloscope. The quality factor for the device is calculated as the ratio of resonant frequency at open load condition and difference in frequencies at half the power at resonant frequency. The value of parasitic damping ( $\zeta_T$ ) is the reciprocal of quality factor ( $Q_T$ ) at open load condition as in Eq. (1).

$$Q_T = \frac{1}{2\zeta_T} \dots\dots\dots(1)$$

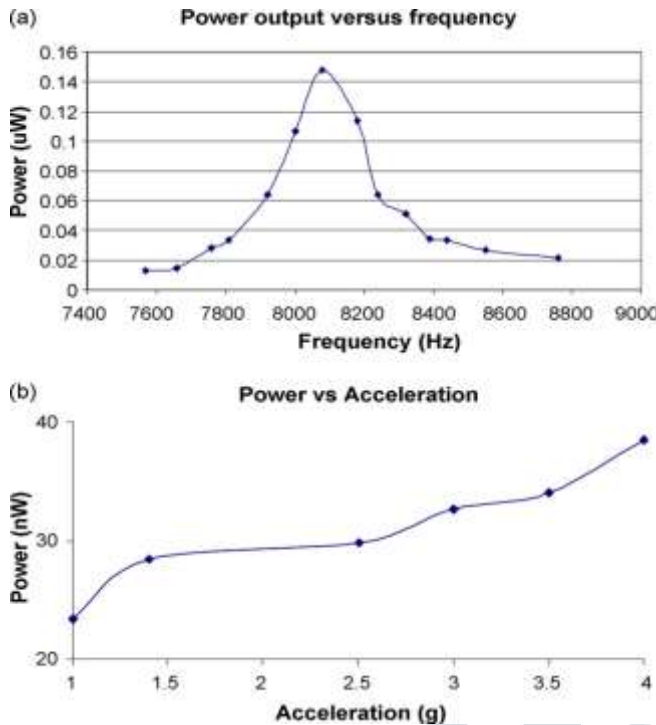


Fig. 7. (a) Variation of load power vs. frequency for Prototype A and (b) variation of load power vs. acceleration for Prototype B.

The variation of power with frequency of Prototype A generator is presented in Fig. 7(a). The value of the maximum power was 148 nW at 8.08 kHz resonant frequency and 3.9 m/s<sup>2</sup> acceleration. The quality factor for the device was measured as 26. For Prototype B, the resonant frequency was observed at 9.837 kHz. The quality factor, *Q*, for the device was 164. The power extracted from the device was about 23 nW for an acceleration of 9.81 m/s<sup>2</sup> into a 52.7 load resistance. The output power was measured at different acceleration levels, up to 39 m/s<sup>2</sup>, for the same load resistance. Fig. 7(b) shows the variation of output power with the acceleration levels. The maximum power output from the device was 40 nW at acceleration of 39.24 m/s<sup>2</sup> for a load resistance of 52.7. The reason for the low output power from the device could be due to lower amplitude of the paddle and the beam. The low amplitude of vibration may be due to a high value of parasitic damping. For Prototype A, the high parasitic damping was due to the friction between the leads of the wire-wound coil and the Perspex lid. The high parasitic damping in case of Prototype B is under investigation.

As mentioned earlier the generators were designed to operate at 7400 Hz as measured in an industrial fan. In practice, the resonant frequency of the generators was 8.08 kHz and 9.8 kHz. This increase in frequency over the design value was due to variations in the fabrication process which

resulted in the dimensions of the fabricated devices being different from the design. However, as the values of parasitic damping in the silicon-based generators reported here are very high, we needed higher values of acceleration to vibrate the paddle and beam. For high values of parasitic damping, most of input energy is required to keep the paddle and beam vibrating; available energy for electrical power generation is not large enough to produce significant levels of power and voltage.

Hence, to verify the potential of electromagnetic power generator using integrated coils, Prototype C was assembled. As mentioned earlier, Serre et al. [5], have reported performance of similarly arranged generator, with moving magnets and fixed nano-fabricated coils. Their generator produced a maximum power of 200 nW at 360 Hz for a vibrational displacement of 6.8 μm. In case of Prototype C, the resonant frequency was found to be around 60 Hz. Fig. 8 shows the variation of load voltage (peak-peak) and load power with load resistance. Here, the acceleration was kept constant at 8.829 m/s<sup>2</sup>. From Fig. 8, Prototype C generates a maximum power of 584 nW and load voltage of 23.5 mV (peak-peak) at a load resistance of 110 (R<sub>load</sub> = 110). At resonance and open load condition, the beam was estimated to move by a maximum displacement of 1.5 mm. In this condition, the only damping present in the device is the parasitic damping, whose value can be calculated from the equation given below

$$Z_{\max} = \frac{ma}{D2\pi f_{\text{res}}} \quad (2)$$

Where *m* is the mass of the beam, *a* the acceleration, *D* the total damping (in this case parasitic damping) and *f<sub>res</sub>* is the resonant frequency. The value of parasitic damping is calculated to be 0.0084 Ns/m. For an electromagnetic power generator, the optimum power condition is reached when the values of parasitic and electromagnetic damping are equal [12]. The electromagnetic damping can be calculated from,

$$D_{\text{em}}(Z) = \left(\frac{d\phi}{dZ}\right)^2 \frac{N^2}{R_{\text{coil}} + R_{\text{load}}} \quad (3)$$

here *dφ/dZ* is the flux gradient and *N* is the number of coil turns. The value of flux gradient per turn from finite element analysis is 1.063 × 10<sup>-3</sup> Wb/m. Using this in Eq. (3), the maximum electromagnetic damping per coil is 4.34 × 10<sup>-5</sup> Ns/m for R<sub>load</sub> = 0. The value of electromagnetic damping decreases with increasing R<sub>load</sub>, with other parameters remaining the same. In this case, as the value of electromagnetic damping is low compared to parasitic

damping, the electromagnetic damping cannot be increased to equal the parasitic damping, to reach the optimum power condition. Here, the displacement given by Eq. (2) is determined by parasitic damping only. In this case, the load power is obtained from the voltage division between the coil and the load. Hence, maximum power is generated across the load, when the load and the coil resistance are equal [12]. This can be seen from Fig. 8, the maximum power of 586nW is transferred across load when the load resistance equals coil resistance ( $R_l = R_c = 110$ ). Table 1 summarizes the experimental results from Prototype A, B and C.

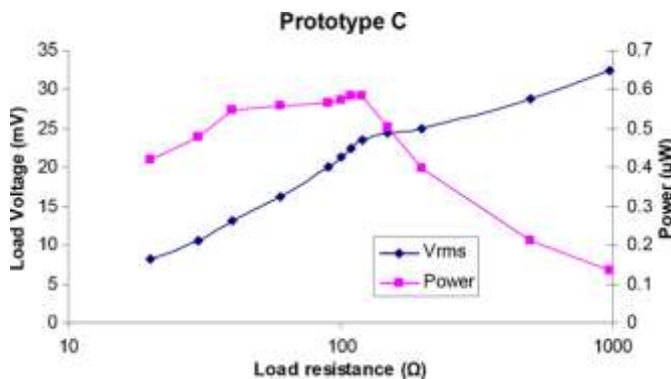


Fig. 8. Variation of load resistance with load voltage and load power for Prototype C.

#### IV. CONCLUSION

This paper describes the design, fabrication and the test results of three types of electromagnetic nanopower generators on silicon. Prototype A uses a wire-wound coil placed in DRIE etched silicon paddle (partially batch-fabricated), Prototype B uses an electrodeposited Cu coils on silicon paddle (fully batch-fabricated). Prototype A and B generators were designed to operate at high frequencies to compensate for low coil turns. The test results of the devices have been reported, for Prototype A, the maximum power output measured was 148nW at 8.08 kHz resonant frequency and 3.9 m/s<sup>2</sup> acceleration. Similarly, for Prototype B, the resonant frequency was measured at 18.83 kHz. At this frequency, the microgenerator gave a maximum load power of 23nW for acceleration of 9.8 m/s<sup>2</sup>, at a load resistance of 52.7. This is a substantial improvement in power generated over other nano-fabricated silicon-based generators reported in literature. The generators have a volume of 0.1 cm<sup>3</sup> which is the lowest of all silicon-based nano-fabricated electromagnetic power generators reported. Still the value of parasitic damping is too large in case of silicon-based generators. Hence, most of the input power is used in keeping the beam vibrating leaving a small portion for electrical power generation. The performance of

electromagnetic power generators using integrated coil was improved using a different design. Prototype C has two oppositely polarized NdFeB on beryllium copper beam placed between two electroplated copper coil on silicon. This generated a maximum power of 586nW measured across a 110 load resistance at a frequency of 60Hz and acceleration of 8.829 m/s<sup>2</sup>.

#### REFERENCES

- [1] S.P. Beeby, M.J. Tudor, N.M. White, Energy harvesting vibration sources for microsystems applications, *Meas. Sci. Technol.* 17 (2006) R175–R195.
- [2] S.P. Beeby, R.N. Torah, M.J. Tudor, P. Glynn-Jones, T. O'Donnell, C.R.Saha, S. Roy, Micro electromagnetic generator for vibration energy harvesting, *J. Micromech. Microeng.* 17 (7) (2007) 1257–1265.
- [3] M. El-Hami, P. Glynn-Jones, E. James, S.P. Beeby, N.M. White, A.D. Brown, J.N. Ross, M. Hill, Design and fabrication of new vibration of a new vibration-based electromechanical power generator, *Sens. Actuators A* 92 (2001) 335–342.
- [4] P. Glynn-Jones, M.J. Tudor, S.P. Beeby, N.M. White, An electromagnetic, vibration-powered generator for intelligent sensor systems, *Sens. Actuators A* 110 (2004) 344–349.
- [5] C. Serre, A. Perez Rodriguez, N. Fondevilla, J.R. Morante, J. Montserrat, J. Esteve, Vibrational energy scavenging with Si technology electromagnetic inertial microgenerators, *Microsyst. Technol.* 13 (11/12) (2007) 1655–1661.
- [6] M. Mizuno, D. Chetwynd, Investigation of a resonance microgenerator, *J. Micromech. Nanoeng.* 13 (2003) 209–216.
- [7] H. Kulah, K. Najafi, An electromagnetic nano power generator for low frequency environmental vibrations, in: *Proceedings of the 17th IEEE Conference on Nano-Electro Mechanical Systems (NEMS)*, Maastricht, 2004, pp. 237–240.
- [8] S.P. Beeby, M.J. Tudor, E. Koukharenko, N.M. White, T. O'Donnell, C.Saha, S. Kulkarni, S. Roy, Nano machined silicon generator for harvesting power from vibrations, in: *Proceedings of 4th International Workshop on Nano and Nanotechnology for Power Generation and Energy*

Conversion Application: Power NEMS, Kyoto, Japan, November 28–30,2004.

[9]S.Kulkarni, S. Roy, T. O'Donnell, S. Beeby, J. Tudor, Vibration-based electromagnetic micropower generator, J. Appl. Phys. 99 (8) (2006) 08P511.

[10] S. Kulkarni, S. Roy, Development of nanostructured, stress-free Co-rich CoPtP films for magnetic nanoelectromechanical system applications, J.Appl. Phys. 101 (2007) 09K524.

[11] E. Koukharenko, S. Beeby, J. Tudor, N. White, T. O'Donnell, C. Saha,S. Kulakrni, S. Roy, NEMS vibration powered electromagnetic generator for wireless sensor applications, micro syst. Technol. 12 (10/11) (2006) 1071–1077.

[12] Gurudutt.C, Sagar Deshpande, Leelavathi NEMS Generator for Nano Vibration Analysis International Symposium on emerging NEMS trends IJCET Trans Magazine 56(15)2011 458-464.

